Stilbene glycoside protects osteoblasts against oxidative damage via Nrf2/HO-1 and NF-κB signaling pathways

Jian Cheng[1], Haohao Wang[2], Zhida Zhang[1], Keyong Liang[1]

[1]The First Department of Orthopedics Ward, First People's Hospital of Yuyao, Yuyao, Zhejiang, China
[2]Department of Tumor Surgery, First Hospital of Zhejiang Province, Hangzhou, Zhejiang, China

Submitted: 23 September 2017
Accepted: 19 November 2017

Arch Med Sci 2019; 15, 1: 196–203
DOI: https://doi.org/10.5114/aoms.2018.79937

Corresponding author:
Jian Cheng
The First Department of Orthopedics Ward
First People's Hospital of Yuyao
Yuyao, Zhejiang
315400, China
E-mail: jianncheng@163.com

Abstract

Introduction: Oxidative stress is currently proposed as a risk factor associated with the development and progression of osteoporosis. Here, the effect of 2,3,5,4'-tetrahydroxystilbene-2-O-β-D-glycoside (THSG) on oxidative damage was investigated in an osteoblast-like MC3T3-E1 cell model.

Material and methods: In this study, MC3T3-E1 cells were treated with hydrogen peroxide (H_2O_2) (100 μM) and THSG (20, 50 and 100 μM), and alkaline phosphatase (ALP). ROS and MDA levels were measured using specific kits. Meanwhile, cell viability and apoptosis were also assessed using MTT methods and flow cytometry, respectively. Then, expression levels of Nrf2 and its downstream targets were determined using real-time PCR and western blotting, as well as the apoptosis related factors, including Bax, Bcl-2, caspase-3, and caspase-9.

Results: Upon H_2O_2 treatment, cell viability was significantly decreased, while THSG clearly attenuated this decrease in a dose-dependent manner. Compared with the negative control, H_2O_2 significantly decreased ALP and increased the levels of MDA, ROS and apoptosis, while THSG markedly reversed these effects in a dose-dependent manner. Moreover, THSG was identified to reverse the elevation of caspase-3, caspase-9 and Bax and the reduction of Bcl-2 induced by H_2O_2. For the Nrf2 signaling pathway, THSG was also observed to attenuate the up-regulation of Nrf2, HO-1, and NQO1, and the down-regulation of NF-κB induced by H_2O_2.

Conclusions: THSG could significantly attenuate oxidative damage induced by H_2O_2 via the Nrf2/NF-κB signaling pathway, providing new insights for treatments of osteoporosis induced by oxidative injury.

Key words: THSG, osteoblast, oxidative damage, NF-κB, Nrf2/HO-1.

Introduction

Oxidative stress has been proposed as an important parameter associated with the pathogenesis of osteoporosis, and the underlying mechanism of oxidative stress induced regulation of the Nrf2/HO-1 and NF-κB signaling pathway in osteoporosis also has been studied extensively [1, 2]. Increasing evidence reveals that reactive oxygen species (ROS) accumulation leads to oxidative stress under conditions of aging, illnesses, or medicine use, and subsequently suppresses the induction of Nrf/HO-1

and NF-κB signaling pathway activation, contributing to the genesis and progression of osteoporosis [3–5]. Therefore, antioxidants have been adopted as a promising therapeutic strategy for osteoporosis treatment.

Radix polygoni multiflori is the dried root of the polygonum plant *Polygonum multiflorum* Thunb. Recent studies have demonstrated that *Radix polygoni multiflori* exhibits antihyperlipidemic and antiatherosclerotic effects in preliminary research [6, 7]. The beneficial properties of 2,3,5,4'-tetrahydroxystilbene-2-O-β-D-glycoside (stilbene glycoside – THSG), which is regarded as the most important bioactive component of *Radix polygoni multiflori*, have been widely investigated, including its outstanding antioxidant and free radical-scavenging ability. Given these properties, recent studies have suggested that THSG could exert potential preventive and therapeutic effects against some chronic diseases, such as apoplexy, senile dementia (Alzheimer's disease), hyperlipemia, and atherosclerosis [8–10].

As a transcription factor, nuclear factor erythroid 2-related factor 2 (Nrf2) is reported to mediate antioxidant related genes by binding to antioxidant response elements. Meanwhile, it has been reported that the activation of Nrf2 plays an important role in the feedback of attenuated oxidative injury via increasing activity of anti-oxidative related enzymes [11, 12]. In addition, THSG also exhibits beneficial effect on free fatty acid, superoxide anion, and focal ischemia induced tissue injury by mediating the activation of NF-κB and Nrf2 [13, 14].

In this study, the effects of THSG on oxidative damage were investigated in osteoblast-like MC3T3-E1 cells. Meanwhile, the involvement of Nrf2/HO-1 and NF-κB signaling pathways was also explored, with the aim of clarifying the potential mechanisms of THSG-mediated antioxidative protective ability in an MC3T3-E1 cell model.

Material and methods

Cell culture

The MC3T3-E1 cell line, similar to osteoblasts, was purchased from the American Type Culture Collection (ATCC). As it recommended, MC3TC-E1 was maintained in α-minimum essential medium (α-MAM) supplied with 10% fetal bovine serum, 100 U/ml penicillin, and 100 μg/ml streptomycin at 37°C with 5% humidity CO_2.

Cell viability assay

Methylthiazol tetrazolium (MTT) assay was applied in this study to measure cell viability. In total 1×10^5/well MC3T3-E1 cells were cultured in 96-well plates, and treated with different concentrations of THSG (0, 5, 10, 20, 50, 80, and 100 μM) for 6, 12, 24, and 48 h, respectively. THSG (originating from the root of the polygonum plant *Polygonum multiflorum* Thunb, molecular weight 406 and purity above 98.52%, No. 110844-200606) was purchased from the National Institute for the Control of Pharmaceutical and Biological Products (Beijing, China). Then, cells were incubated with 0.5 mg/ml MTT at 37°C for 4 h after washing twice with PBS. Next, 200 μl of dimethyl sulfoxide was added to dissolve the produced formazan salts. An ELISA reader was used to measure the optical density at the wavelength of 490 nm, and the mean value of repeats was calculated.

Alkaline phosphatase (ALP) activity

MC3T3-E1 cells were seeded in a 12-well plate, and then cultured with α-MEM (Basal), H_2O_2 (100 μM), H_2O_2 (100 μM) + THSG (20 μM), H_2O_2 (100 μM) + THSG (50 μM), and H_2O_2 (100 μM) + THSG (100 μM) at 37°C for 4 h. After treatment, fresh medium was used to cultivate these cells for 5 days. Subsequently, cell samples were lysed using lysis buffer centrifuged at 12,000×g for 10 min. Then, supernatant was collected, and ALP activity and protein concentration in the supernatant were determined using the ALP activity assay kit (Cell Biolabs, San Diego, CA, USA) and BCA-protein assay kit (Biyuntian, Nanjing, China), respectively.

Apoptosis

MC3T3-E1 cells were cultured in a 6-well plate, and treated with α-MEM (Basal), H_2O_2 (100 μM), H_2O_2 (100 μM) + THSG (20 μM), H_2O_2 (100 μM) + THSG (50 μM), and H_2O_2 (100 μM) + THSG (100 μM) for 4 h respectively. Annexin V/PI double staining was performed to measure apoptosis according to the manufacturer's instructions. A FACScan flow cytometer (Becton Dickinson, San Jose, CA, USA) was used to assess the percentage of apoptosis cells.

Malondialdehyde (MDA) determination

MC3T3-E1 cells were seeded in a 6-well plate, and treated with α-MEM (Basal), H_2O_2 (100 μM), H_2O_2 (100 μM) + THSG (20 μM), H_2O_2 (100 μM) + THSG (50 μM), and H_2O_2 (100 μM) + THSG (100 μM) for 4 h respectively. The MDA concentration was determined using an MDA assay kit (Cayman, Ann Arbor, USA).

Intracellular ROS determination

MC3T3-E1 cells were seeded in a 6-well plate, and treated with α-MEM (Basal), H_2O_2 (100 μM), H_2O_2 (100 μM) + THSG (20 μM), H_2O_2 (100 μM) + THSG (50 μM), and H_2O_2 (100 μM) + THSG

(100 µM) for 4 h respectively. Intracellular ROS were quantified using the ROS-sensitive dye DCFH-DA.

Real-time PCR

Total RNA was isolated using Trizol reagent (Gibco, Life Technology, Carlsbad, CA, USA) according to the manufacturer's protocol. Reverse transcription reactions were performed as described. Then, mRNA expression was evaluated in real time on the ABI 7500 thermal cycler platform (Applied Biosystems, Foster City, CA, USA), and relative expression levels were evaluated using the $2^{-\Delta\Delta Ct}$ method. Primers for each gene were as follows: 5′-TTCCTCTGCTGCCATTAGTCAGTC-3′ and 5′-GCTCTTCCATTTCCGAGTCACTG-3′ for Nrf2 (product: 215 bps); 5′-ATCGTGCTCGCATGAACACT-3′ and 5′-CCAACACTGCATTTACATGGC-3′ for HO-1 (product: 339 bps); 5′-ACTCGGAGAACTTTCAGTACC-3′ and 5′-TTGGAGCAAAGTAGAGTGGT-3′ for NQO1 3 (product: 492 bps); 5′-ATCACTGCCACCCAGAAG-3′ and 5′-TCCACGACGGACACATTG-3′ for GAPDH.

Western blot analysis

Cells were lysed in ice-cold radio immunoprecipitation assay buffer (RIPA, Beyotime, Shanghai, China) with fresh 0.01% protease inhibitor cocktail (Sigma, Shanghai, China) after treatment. Subsequently, cell lysate was centrifuged (13,000 rcf, 10 min, 4°C), and protein concentration of supernatant was determined using the BCA protein assay kit. Protein (20–30 µg) was loaded onto a 10% SDS-PAGE gel, and then transferred to a PVDF membrane (Millipore, Shanghai, China). For immunodetection, the membrane was blocked with 5% skim milk dissolved in phosphate-buffered saline with 0.05% Tween (PBST) at room temperature for 1 h. Then, blots were probed with primary antibodies against pro-caspase-3/-9, caspase-3/-9, Bcl-2, Bax, NF-κB, Nrf2, HO-1, NQO1 and GAPDH overnight, washed with PBST for 5 min and repeated 3 times. Blot membranes were incubated with goat anti-mouse or anti-rabbit secondary antibody (Beyotime, Shanghai, China). After washing with PBST, blots were visualized using the enhanced chemiluminescence method. GAPDH was used as the internal standard for western blotting.

Statistical analysis

Continuous data were presented as mean ± standard deviation (SD). Comparisons between groups were measured using Student's *t* test. The difference was considered as statistically significant when $p < 0.05$ ($^*p < 0.05$, $^{**}p < 0.01$, $^{***}p < 0.005$). Statistical analysis was performed using SAS statistical software (SAS Inc., NC, USA).

Results

Effects of THSG on cell viability of MC3T3-E1 cells

To identify the effect of THSG on proliferation of MC3T3-E1 cells, the MTT assay was carried out. As shown in Figure 1, after treatment with THSG (at 0, 5, 10, 20, 50, 80, and 100 µM) for 6, 12, 24 and 48 h, THSG over the dose of 20 µM could obviously increase the cell viability of MC3T3-E1 cells at 6, 12, 24 and 48 h in a dose- and time-dependent manner. Based on the promotive effects of THSG on cell viability, concentrations of 20, 50, and 100 µM of THSG were determined for the further investigations.

Effects of THSG on ALP activity, MDA, and ROS in H_2O_2-insulted MC3T3-E1 cells

Serum alkaline phosphatase (ALP) is recognized as one of the bone formation markers. In MC3T3-E1 cells, ALP activity could be significantly decreased in H_2O_2 treated cells compared with the controls ($^*p < 0.05$). However, THSG significantly increased the ALP level in a dose-dependent manner ($^{**}p <$

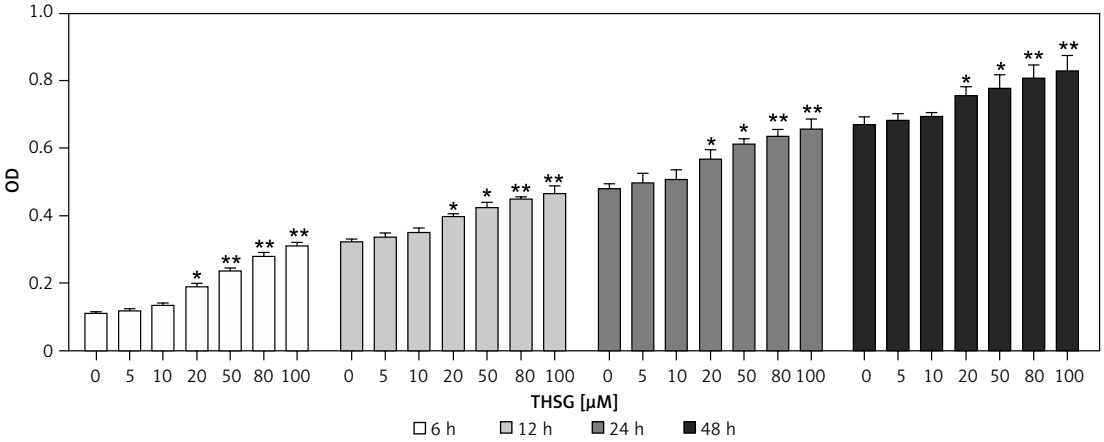

Figure 1. Effect of THSG on MC3T3-E1 cell viability. After treatment with various concentrations of THSG (0, 5, 10, 20, 50, 80 and 100 µM) for 6, 12, 24 and 48 h, MC3T3-E1 cell viability was assessed using the MTT assay as described in Material and methods (error bar = ± SD, $n = 6$, $^*p < 0.05$, $^{**}p < 0.01$)

0.05, Figure 2 A). Meanwhile, the level of MDA was also assessed. The results showed that the MDA level significantly increased after treatment with H_2O_2 (**p < 0.05), while THSG could markedly reverse this elevation in a dose-dependent manner (**p < 0.05, Figure 2 B). These findings suggested that THSG might play an obviously negative role in the regulation of H_2O_2 induced oxidative damage. Thus, ROS levels in MC3T3-E1 cells with different treatments were measured. The results showed that the ROS level was significantly increased upon H_2O_2 treatment, but THSG intervention could markedly reduce ROS levels increased by H_2O_2 in a dose-dependent manner (Figure 3).

Effects of THSG on apoptosis of H_2O_2-insulted MC3T3-E1 cells

To further investigate the effect of THSG on apoptosis, H_2O_2 treatments were carried out using MC3T3-E1 cells. Flow cytometric results showed that H_2O_2 significantly promoted cell apoptosis, while THSG treatment could evidently reverse this elevation in a dose-dependent manner (Figure 4).

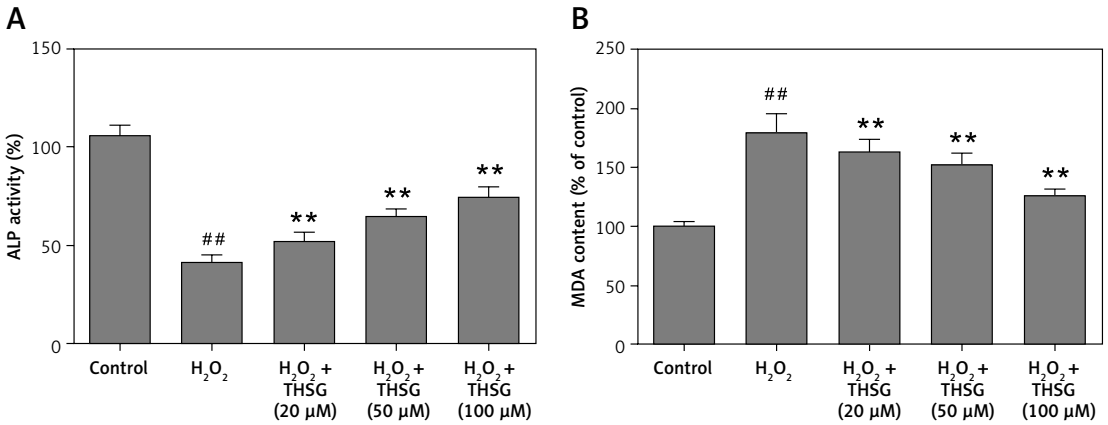

Figure 2. Effect of THSG on ALP and MDA in MC3T3-E1 cells. **A** – THSG attenuated decreased ALP activity induced by H_2O_2 treatment; **B** – THSG reversed the elevation of MDA induced by H_2O_2 treatment. In this experiment, treatments of different groups are designed as follows: control, H_2O_2 (100 μM), H_2O_2 + THSG (20 μM), H_2O_2 + THSG (50 μM), and H_2O_2 + THSG (100 μM) (error bar = ± SD, *p < 0.05, **p < 0.01, ##p < 0.01)

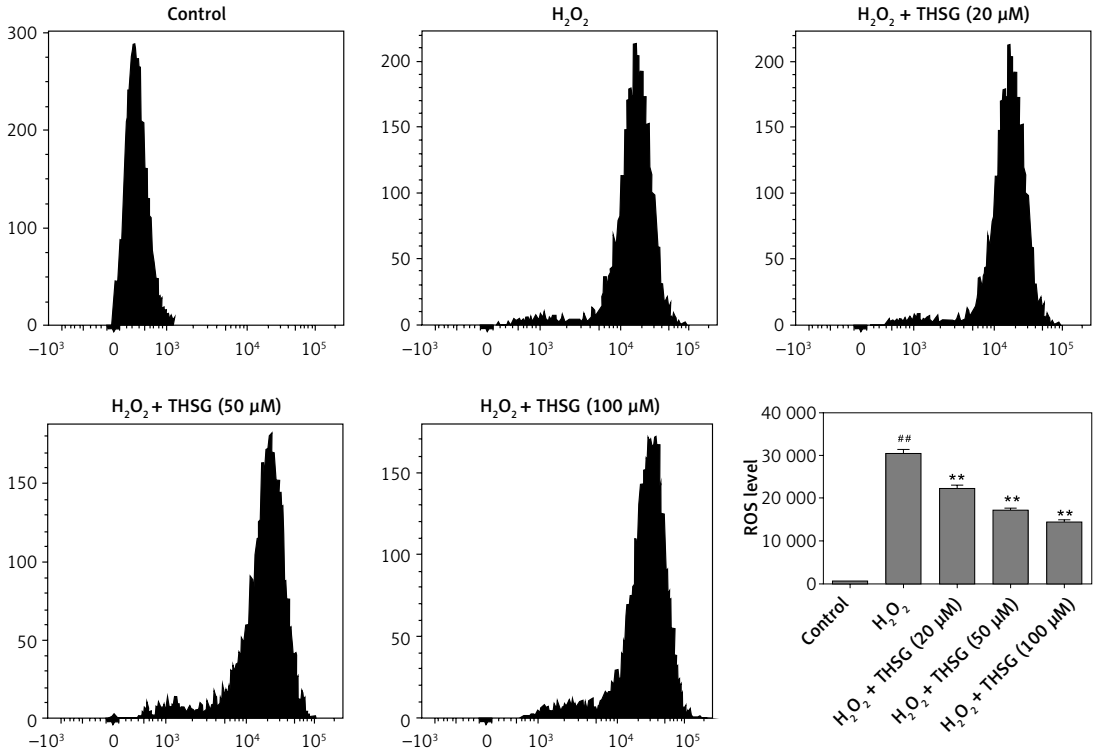

Figure 3. THSG attenuated the elevation of ROS level in H_2O_2-insulted MC3T3-E1 cells. Cells treated with control, H_2O_2 (100 μM), H_2O_2+ THSG (20 μM), H_2O_2+ THSG (50 μM) and H_2O_2 + THSG (100 μM). ROS levels were identified by flow cytometry (error bar = ± SD, n = 6, *p < 0.05, **p < 0.01, ##p < 0.01)

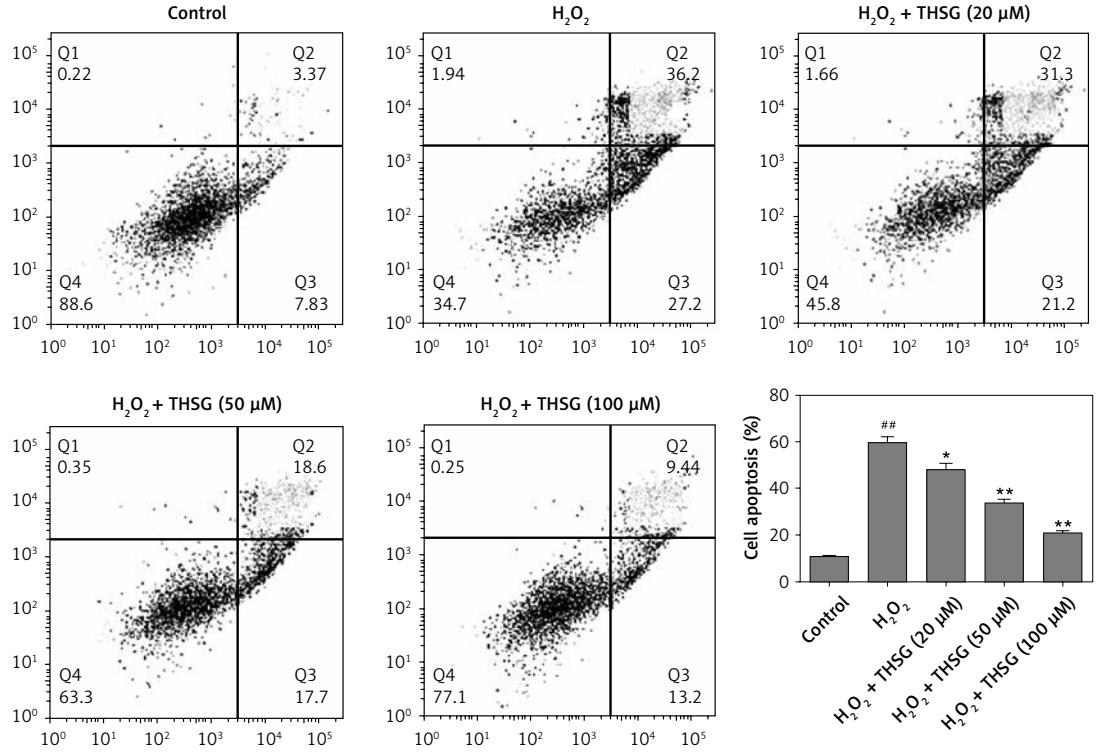

Figure 4. Effect of THSG on apoptosis in H_2O_2 treated MC3T3-E1 cells. Cells treated with control, H_2O_2 (100 μM), H_2O_2 + THSG (20 μM), H_2O_2 + THSG (50 μM), and H_2O_2 + THSG (100 μM). Annexin V assay was used for apoptosis detection (error bar = ± SD, $n = 6$, $^{*}p < 0.05$, $^{**}p < 0.01$, $^{\#\#}p < 0.01$)

Meanwhile, apoptosis related protein levels were also detected. The western blotting results showed that H_2O_2 treatment significantly up-regulated the expression levels of caspase-3, caspase-9, and Bax, and markedly down-regulated the expression of Bcl-2, while THSG could obviously reverse these effects in a dose-dependent manner (Figure 5).

Effects of THSG on Nrf2/HO-1 and NF-κB signaling

To further reveal THSG involved signaling pathways, expression levels of Nrf2 and its downstream effectors were evaluated using RT-PCR and western blot. RT-PCR results showed that the expression levels of Nrf2, HO-1, and NQO1 were significantly decreased after treatment with H_2O_2, while THSG intervention could significantly reverse these elevations (Figure 6 A). Meanwhile, protein levels of Nrf2, HO-1 and NQO1 as well as NF-κB were also measured. The western blotting results showed that the protein expression levels of Nrf2, HO-1, and NQO1 were significantly lower in the H_2O_2 treated group than in the control group, while THSG significantly increased the expression levels of Nrf2, HO-1, and NQO1 in a dose-dependent manner (Figures 6 B, D). However, the expression level of NF-κB significantly increased in the H_2O_2 treated group compared to the negative control, and THSG could obviously reverse this increase, which was contrary to the variations of Nrf2 and its downstream target (Figure 6 C, D).

Discussion

In the present study, the bio-functional effects of THSG on oxidative damage were investigated in MC3T3-E1 cells. The results showed that THSG protected osteoblasts against oxidative damage via attenuating cell apoptosis and oxidative stress, thereby promoting cell viability. Further analysis demonstrated that the protective effect might be developed via regulating Nrf2 and NF-κB signaling pathways.

Oxidative stress acts as an important pathogenic factor for age related bone loss by regulating osteoblast and osteocyte apoptosis, osteoblast numbers, etc [15–17]. Moreover, oxidative stress has a close relationship with the pathogenesis of osteoporosis [18–20]. Statistics display a strong dependency between higher oxidative stress and lower bone mineral density in ≥ 55-year-old patients [21]. *In vitro* studies demonstrated that H_2O_2 can mediate osteoblastic differentiation, and promoted osteoblastic apoptosis. Several bone formation related metabolic markers such as ALP have been applied to investigate the effects of THSG on pathogenesis. [22]. In this study, THSG was identified to have the ability to revise the increase of apoptosis and ROS and decrease of ALP activity induced by H_2O_2 treatment. Mitochondria

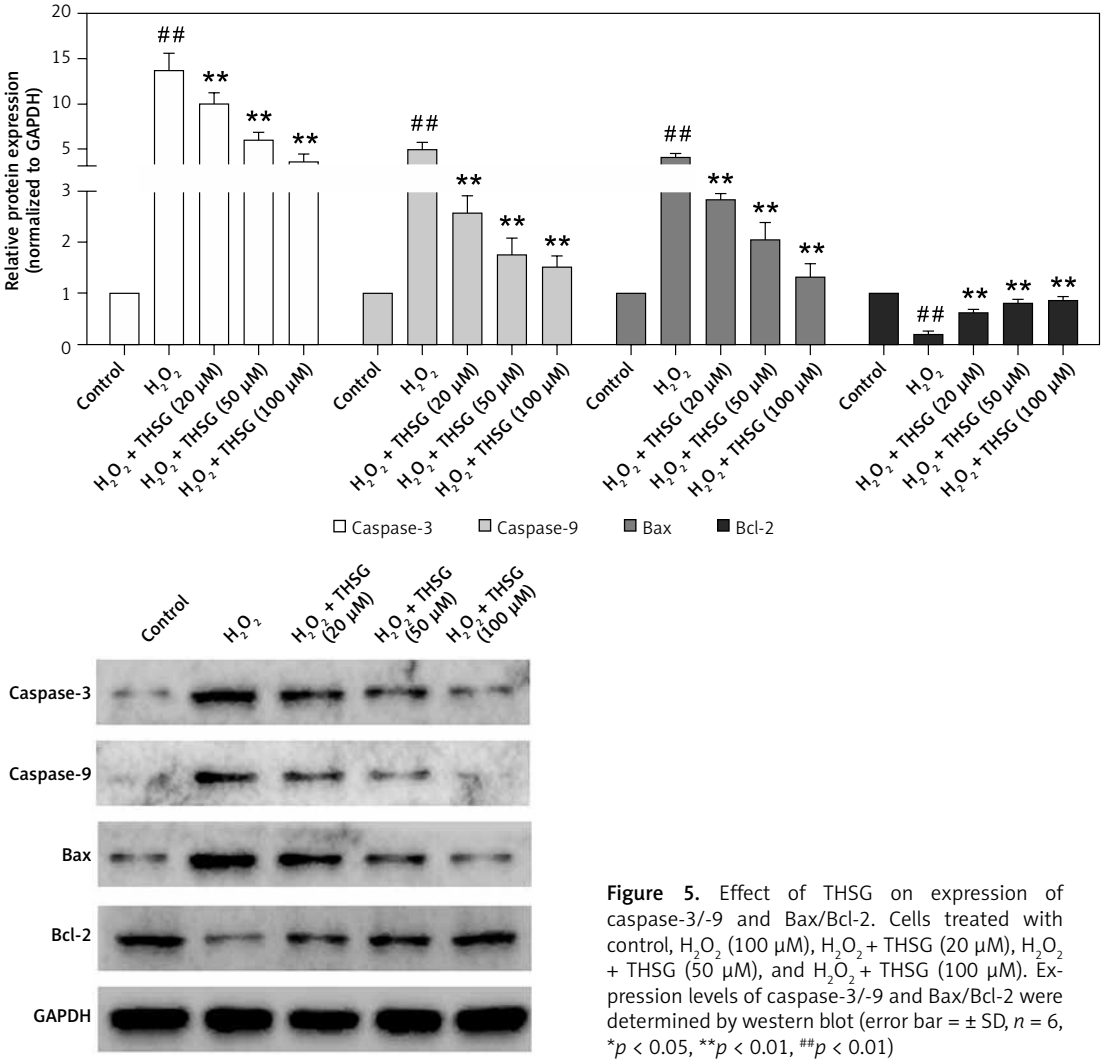

Figure 5. Effect of THSG on expression of caspase-3/-9 and Bax/Bcl-2. Cells treated with control, H_2O_2 (100 μM), H_2O_2 + THSG (20 μM), H_2O_2 + THSG (50 μM), and H_2O_2 + THSG (100 μM). Expression levels of caspase-3/-9 and Bax/Bcl-2 were determined by western blot (error bar = ± SD, $n = 6$, $^{*}p < 0.05$, $^{**}p < 0.01$, $^{\#\#}p < 0.01$)

are critical for mediating the complex process of apoptosis. During this process, cytochrome c was released from mitochondria, and then interacted with caspase-9, which subsequently activate caspase-3 [23, 24] to further develop the process of apoptosis. Bcl-2 family members, including anti-apoptotic proteins and pro-apoptotic proteins, are crucial for regulating the mitochondrial death pathway [25, 26]. As an anti-apoptosis protein, Bcl-2 is located on the outer mitochondrial membrane to maintain mitochondrial permeability and to suppress cytochrome *c* release. In this study, expression of caspase-3, caspase-9, and Bax was significantly increased, and Bcl-2 significantly decreased after H_2O_2 treatment compared with the negative control, while THSG treatment could markedly reverse these changes, indicating that THSG could protect the MC3T3-E1 cells against the caspase-mitochondrial death pathway induced by oxidative stress.

The Nrf2 signaling pathway has been demonstrated as the major regulator in the meditation of endogenous and exogenous stresses induced by ROS and electrophiles [11, 27]. Thus, we explored the effects of H_2O_2 on the protein expression of Nrf2 and its downstream genes, including HO1 and NQO1, by RT-PCR and western blot. The results showed that Nrf2, HO1 and NQO1 were dramatically attenuated upon H_2O_2 treatment, and significantly up-regulated after THSG treatments. NF-κB is a negative regulator of Nrf2 expression and participates in oxidative injury induced by H_2O_2 [28, 29]. In this study, THSG was significantly identified to revise the decrease of Nrf2 expression and increase of NF-κB p65 in H_2O_2 treated cells, indicating that THSG could resist oxidative damage by regulating Nrf2 and NF-κB signaling pathways.

Collectively, THSG could attenuate oxidative injury induced by H_2O_2 in osteoblasts via NF-κB and Nrf2 signaling pathways. These findings might provide a possible protocol for treatment of osteoporosis, which needs an in-depth study at the molecular and cellular level to further demonstrate how THSG reduces oxidant generative diseases.

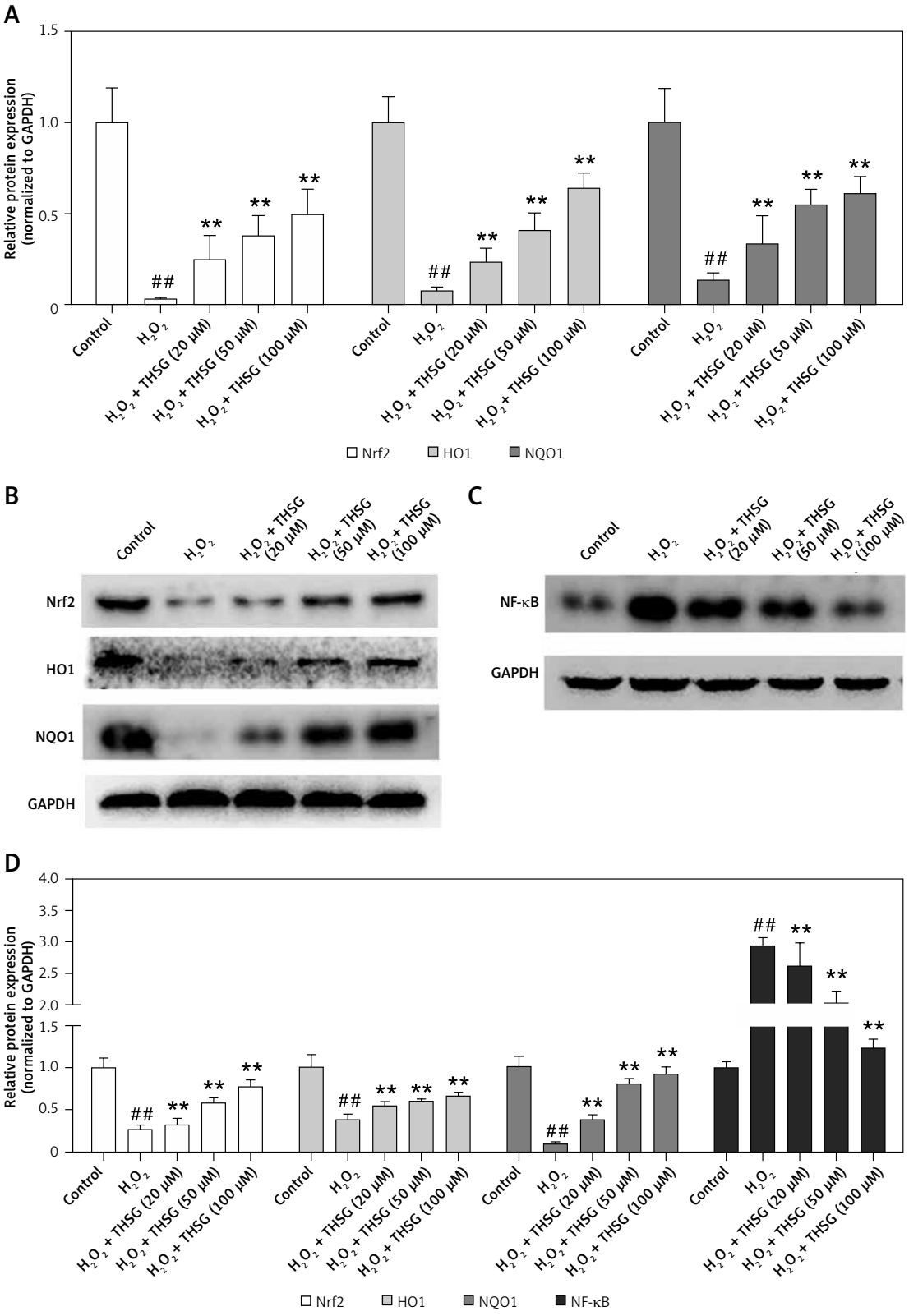

Figure 6. Effect of THSG on expression of Nrf2 and NF-κB pathway. **A** – mRNA expression levels of Nrf2, NQO1 and HO1 determined using real-time PCR. **B** – Protein expression of Nrf2, NQO1 and HO1 determined using western blotting. **C** – Protein expression of NF-κB determined using western blotting. **D** – Quantification of western blotting results of Nrf2, NQO1, HO1 and NF-κB. In this experiment, treatments of different groups are designed as follows: control, H_2O_2 (100 μM), H_2O_2 + THSG (20 μM), H_2O_2 + THSG (50 μM), and H_2O_2 + THSG (100 μM) (error bar = ± SD, $n = 6$, $^{*}p < 0.05$, $^{**}p < 0.01$, $^{\#\#}p < 0.01$)

Conflict of interest

The authors declare no conflict of interest.

References

1. Mak JC. Acupuncture in osteoporosis: more evidence is needed. Acupunct Med 2015; 33: 440-1.
2. Tanaka Y, Mori H, Aoki T, et al. Analysis of bone metabolism during early stage and clinical benefits of early intervention with alendronate in patients with systemic rheumatic diseases treated with high-dose glucocorticoid: Early DIagnosis and Treatment of OsteopoRosis in Japan (EDITOR-J) study. J Bone Miner Metab 2015; 34: 646-54.
3. Weaver CM, Alexander DD, Boushey CJ et al. Calcium plus vitamin D supplementation and risk of fractures: an updated meta-analysis from the National Osteoporosis Foundation. Osteoporos Int 2016; 27: 367-76.
4. Chen K, Zhang N, Ding L, Zhang W, Hu J, Zhu S. Early intra-articular injection of alendronate reduces cartilage changes and subchondral bone loss in rat temporomandibular joints after ovariectomy. Int J Oral Maxillofac Surg 2014; 43: 996-1004.
5. Schmid T, Brumme UM, Kemerle S, Zimmer K. Elderly osteoporosis suspects without diagnosis – interim data from a German Geriatric Practice. Value Health 2015; 18: A654.
6. Lin P, He YR, Lu JM, et al. In vivo lipid regulation mechanism of polygoni multiflori radix in high-fat diet fed rats. Evid Based Complement Alternat Med 2014; 2014: 642058.
7. Ma J, Zheng L, Deng T, et al. Stilbene glucoside inhibits the glucuronidation of emodin in rats through the down-regulation of UDP-glucuronosyltransferases 1A8: application to a drug-drug interaction study in Radix Polygoni Multiflori. J Ethnopharmacol 2013; 147: 335-40.
8. Xiang K, Liu G, Zhou YJ, et al. 2,3,5,4'-tetrahydroxystilbene-2-O-beta-D-glucoside (THSG) attenuates human platelet aggregation, secretion and spreading in vitro. Throme Res 2014; 133: 211-7.
9. Tamura M, Koshibe Y, Kaji K, Ueda JY, Shirataki Y. Attempt to synthesize 2,3,5,4'-tetrahydroxystilbene derived from 2,3,5,4'-tetrahydroxystilbene-2-O-beta-glucoside (THSG). Chem Pharm Bull (Tokyo) 2015; 63: 122-5.
10. Zeng C, Xiao JH, Chang MJ, Wang JL. Beneficial effects of THSG on acetic acid-induced experimental colitis: involvement of upregulation of PPAR-gamma and inhibition of the Nf-kappaB inflammatory pathway. Molecules 2011; 16: 8552-68.
11. McMahon M, Campbell KH, MacLeod AK, McLaughlin LA, Henderson CJ, Wolf CR. HDAC inhibitors increase NRF2-signaling in tumor cells and blunt the efficacy of co-adminstered cytotoxic agents. Plos One 2014; 9: e114055.
12. Vurusaner B, Gamba P, Gargiulo S, et al. Nrf2 antioxidant defense is involved in survival signaling elicited by 27-hydroxycholesterol in human promonocytic cells. Free Radic Biol Med 2015; 91: 93-104.
13. Ren X, Ouyang H, Wang G, Zhao M, Qi A. Study on excretion of stilbene glycoside (THSG) and its beta-cyclodextrin inclusion. Zhongguo Zhong Yao Za Zhi 2010; 35: 2620-3.
14. Ye S, Tang L, Xu J, Liu Q, Wang J. Postconditioning's protection of THSG on cardiac ischemia-reperfusion injury and mechanism. J Huazhong Univ Sci Technolog Med Sci 2006; 26: 13-6.
15. Jiao L, Cao DP, Qin LP, et al. Antiosteoporotic activity of phenolic compounds from Curculigo orchioides. Phytomedicine 2009; 16: 874-81.
16. Guo CC, Zheng LH, Fu JY, et al. Antiosteoporotic effects of huangqi sanxian decoction in cultured rat osteoblasts by proteomic characterization of the target and mechanism. Evid Based Complement Alternat Med 2015; 2015: 514063.
17. Jian J, Sun L, Cheng X, Hu X, Liang J, Chen Y. Calycosin-7-O-beta-glucopyranoside stimulates osteoblast differentiation through regulating the BMP/WNT signaling pathways. Acta Pharm Sin B 2015; 5: 454-60.
18. Wu Q, Zhong ZM, Pan Y, et al. Advanced oxidation protein products as a novel marker of oxidative stress in postmenopausal osteoporosis. Med Sci Monit 2015; 21: 2428-32.
19. Demir M, Ulas T, Tutoglu A, et al. Evaluation of oxidative stress parameters and urinary deoxypyridinoline levels in geriatric patients with osteoporosis. J Phys Ther Sci 2014; 26: 1405-9.
20. Yang YH, Li B, Zheng XF, et al. Oxidative damage to osteoblasts can be alleviated by early autophagy through the endoplasmic reticulum stress pathway: implications for the treatment of osteoporosis. Free Radic Biol Med 2014; 77: 10-20.
21. Spilmont M, Leotoing L, Davicco MJ, et al. Pomegranate and its derivatives can improve bone health through decreased inflammation and oxidative stress in an animal model of postmenopausal osteoporosis. Eur J Nutr 2014; 53: 1155-64.
22. Phillips JE, Gersbach CA, Wojtowicz AM, Garcia AJ. Glucocorticoid-induced osteogenesis is negatively regulated by Runx2/Cbfa1 serine phosphorylation. J Cell Sci 2006; 119: 581-91.
23. Mattiolo P, Yuste VJ, Boix J, Ribas J. Autophagy exacerbates caspase-dependent apoptotic cell death after short times of starvation. Biochem Pharmacol 2015; 98: 573-86.
24. Liu XR, Li YQ, Hua C, et al. Oxidative stress inhibits growth and induces apoptotic cell death in human U251 glioma cells via the caspase-3-dependent pathway. Eur Rev Med Pharmacol Sci 2015; 19: 4068-75.
25. Sumitani M, Sakurai T, Kasashima K, et al. Establishment of a specific cell death induction system in Bombyx mori by a transgene with the conserved apoptotic regulator, mouse Bcl-2-associated X protein (mouse Bax). Insect Mol Biol 2015; 24: 671-80.
26. Park JA, Jin HO, Lee HN, et al. S6K1 inhibition enhances the apoptotic cell death of breast cancer cells in response to Bcl-2/Bcl-xL inhibition by the downregulation of survivin. Oncol Lett 2015; 10: 829-34.
27. Roy CS, Sengupta S, Biswas S, et al. Bacterial fucose-rich polysaccharide stabilizes MAPK-mediated Nrf2/Keap1 signaling by directly scavenging reactive oxygen species during hydrogen peroxide-induced apoptosis of human lung fibroblast cells. Plos One 2014; 9: e113663.
28. Wang P, Qiao Q, Li J, Wang W, Yao LP, Fu YJ. Inhibitory effects of geraniin on LPS-induced inflammation via regulating NF-kappaB and Nrf2 pathways in RAW 264.7 cells. Chem Biol Interact 2016; 253: 134-42.
29. Jang HJ, Hong EM, Kim M, et al. Simvastatin induces heme oxygenase-1 via NF-E2-related factor 2 (Nrf2) activation through ERK and PI3K/Akt pathway in colon cancer. Oncotarget 2016; 7: 46219-29.